Trends in Applied Sciences Research

ISSN 1819-3579

Academic
Journals Inc.

www.academicjournals.com

Trends in Applied Sciences Research 1 (1): 15-24, 2006
ISSN 1819-3579

Electrochemical Properties of Cathode Materials $LiNiO_2$ and $LiNi_{1-y}M_yO_2$ ($M = Zn^{2+}$, Al^{3+} and Ti^{4+})

M.Y. Song and D.S. Lee
Division of Advanced Materials Engineering,
Research Center of Advanced Materials Development,
Engineering Research Institute,
Chonbuk National University,
664-14 1ga Deogjindong Deogjingu Jeonju 561-756,
Republic of Korea

Abstract: $LiNi_{1-y}Ti_yO_2$ (y = 0.000, 0.012, 0.025, 0.050, 0.100 and 0.150) were synthesized by ball milling and the solid- state reaction method. The optimum condition to synthesize a cathode material $LiNi_{0.975}Ti_{0.025}O_2$ is milling for 28 h and then preheating at 600°C for 16 h and finally calcining at 750°C for 30 h O_2 stream. $LiNi_{1-y}Ti_yO_2$ ($0 \le y \le 0.150$) synthesized under this optimum condition have the α-$NaFeO_2$ structure of the rhombohedral system (space group; $R\bar{3}m$). The values of I_{003}/I_{104} for y = 0.000, 0.012 and 0.025 are near 1.2, indicating these samples have the phase with the nearly stoichiometric composition. The samples with y = 0, 0.012 and 0.025 show good splitting of 006 and 102 peaks and of 108 and 110 peaks, indicating the decrease in cation mixing. The particle size decreases as the value of y increases. All the samples except that with y = 0.000 exhibit relatively homogeneous particle size. The voltage vs. discharge capacity curves for y = 0.012 and y = 0.025 exhibit three distinct plateaus corresponding to phase transitions. Among $LiNi_{1-y}Ti_yO_2$ ($0 = y = 0.150$), $LiNi_{0.975}Ti_{0.025}O_2$ has the largest first discharge capacity 154.8mAhg^{-1} and the relatively good cycling performance (77% at n = 10). For Ti in the composition $LiNi_{0.975}Ti_{0.025}O_2$, Zn^{2+} and Al^{3+} were substituted. Electrochemical studies of $LiNi_{0.975}M_{0.025}O_2$ ($M = Zn^{2+}$, Al^{3+} and Ti^{4+}) show that the plateaus in the voltage vs. discharge capacity curve become more distinct and the voltage of the plateau corresponding to the phase transition from M to H_1 increases as M varies from Zn^{2+} to Al^{3+} and then to Ti^{4+}. $LiNi_{0.975}Ti_{0.025}O_2$ has the largest first discharge capacity and a relatively good cycling performance compared with $LiNi_{0.975}M_{0.025}O_2$ ($M = Zn^{2+}$ and Al^{3+}). This sample has the largest value of c/a and the smallest particles. $LiNi_{0.975}Al_{0.025}O_2$ has the best cycling performance (98% at n = 10).

Key words: $LiNiO_2$, substitution of Zn^{2+}, Al^{3+} and Ti^{4+}, ball milling, solid-state reaction method, discharge capacity, cycling performance

Introduction

The transition metal oxides such as $LiCoO_2$ (Ozawa, 1994; Alcantara *et al*., 1997; Peng *et al*., 1998), $LiNiO_2$ (Dahn *et al*., 1990; 1991; Marini *et al*., 1991; Ebner *et al*., 1994) and $LiMn_2O_4$ (Tarascon *et al*., 1991; Song and Ahn, 1998; Song *et al*., 1999; Ahn and Song, 2000) have been

Corresponding Author: Song M.Y., Division of Advanced Materials Engineering, Research Center of Advanced Materials Development, Engineering Research Institute, Chonbuk National University, 664-14 1ga Deogjindong Deogjingu Jeonju 561-756, Republic of Korea
Tel: +82-63-270-2379 Fax : +82-63-270-2386

investigated as cathode materials for lithium secondary batteries. $LiMn_2O_4$ is very cheap and does not bring about environmental pollution, but its cycling performance is not good. $LiCoO_2$ has a large diffusivity and a high operating voltage and it can be easily prepared. However, it has a disadvantage that it contains an expensive element, Co. $LiNiO_2$ is a very promising cathode material since it has a large discharge capacity (Nishida *et al*., 1997) and is relatively excellent from the viewpoints of economics and environment. However, its preparation is very difficult as compared with $LiCoO_2$ and $LiMn_2O_4$.

It is known that $Li_{1-x}Ni_{1+x}O_2$ forms rather than stoichiometric $LiNiO_2$ during preparation. This phenomenon is called cation mixing. Excess nickel occupies the Li sites, destroying the ideally layered structure and preventing lithium ions from easy movement for intercalation and deintercalation during cycling. This results in a small discharge capacity and a poor cycling performance. To solve the problem of cation mixing, Co^{3+}, Al^{3+}, Mn^{3+} and Ti^{4+} ions were substituted for lithium ion in $LiNiO_2$ (Gao *et al*., 1998; Broussely, 1990; Caurant *et al*., 1996). According to Amine *et al*. (2002) and Gao *et al*. (1998), the substitution of Ti for Ni resulted in a large discharge capacity and a good cycling performance.

In this study, the optimum conditions to synthesize $LiNiO_2$ were investigated and $LiNi_{1-y}M_yO_2$ (M = Zn^{2+}, Al^{3+} and Ti^{4+}, y = 0.005, 0.01, 0.025, 0.05 and 0.1) were synthesized under the optimum conditions for the synthesis of $LiNiO_2$. In addition their electrochemical properties were measured.

Materials and Methods

$LiOH{\bullet}H_2O$ (Aldrich Co., purity 98%), $Ni(OH)_2$ (Aldrich Co., purity 99%), ZnO (Aldrich Co., purity 99.9%), $Al(OH)_3$ (High Purity Chemical Laboratory Co., purity 99.99%) and TiO_2 (anatase)(Aldrich Co., purity 99%) were used as starting materials in order to synthesize $LiNi_{1-y}M_yO_2$ by ball milling and solid-state reaction method.

The experimental procedure of this work is given schematically in Fig. 1. Mixtures of starting materials in the compositions $LiNi_{1-y}M_yO_2$ were mixed by ball milling in acetone and dried in a drying oven. They were then preheated at 600°C for 16 h in air and palletized. This pellet was heated in a heating rate 50°C h^{-1} and calcined at 750, 800 and 850°C for 30 h in O_2 stream. Then it was cooled in a cooling rate 100°C h^{-1}.

The phase identification of the synthesized samples was carried out by X-ray Diffraction (XRD) analysis using Cu-K_α radiation. The X-ray diffractometer was Rigaku III/A type. The scanning rate was 4°/min and the scanning range of diffraction angle (2θ) was $10° \leq 2\theta \leq 80°$. The morphologies of the samples were observed using a field emission scanning electron microscope (FE-SEM). The particle size distributions and the specific surface areas of the samples were analyzed by a particle size analyzer (Malvern Instruments).

The electrochemical cells consisted of $LiNi_{1-y}M_yO_2$ as a positive electrode, Li foil as a negative electrode and electrolyte [Purelyte (Samsung General Chemicals Co., Ltd.)] prepared by solving 1M $LiPF_6$ in a 1:1(volume ratio) mixture of Ethylene Carbonate (EC) and diethyl carbonate (DEC). A Whattman glass-fiber was used as the separator. The cells were assembled in an argon-filled dry box. To fabricate the positive electrode, 85wt.% synthesized oxide, 10wt.% acetylene black and 5wt.% Polyvinylidene Fluoride (PVDF) binder solved in 1-Methyl-2-pyrrolidinone were mixed. By introducing Li metal, Wattman glass-filter, positive electrode and the electrolyte, the

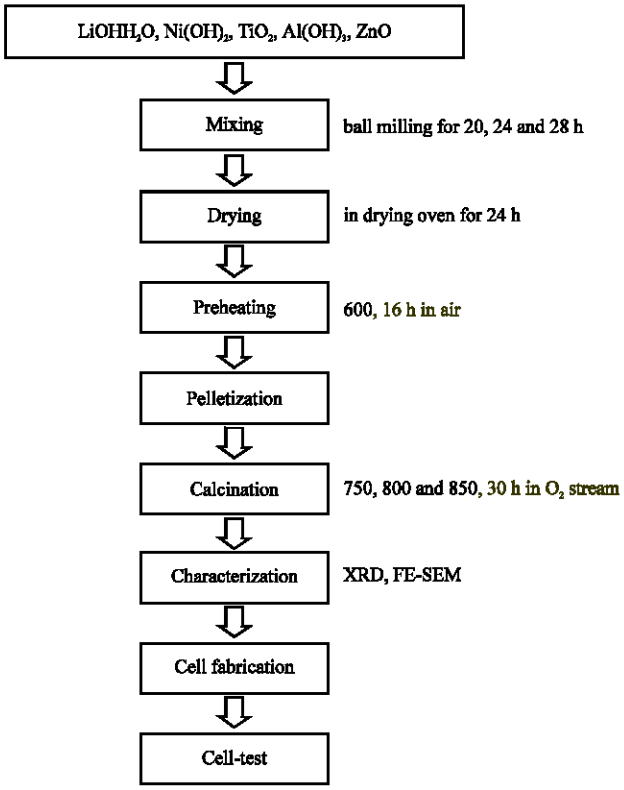

Fig. 1: Schematic diagram of experimental procedure

cell was assembled in a glove box filled with argon. All the electrochemical tests were performed at room temperature with a potentiostatic/galvanostatic system. The cells were cycled at a current density of 193 μA cm^{-2} corresponding to 0.1 C rate between 2.8 and 4.3V.

Results and Discussion

The X-ray diffraction (XRD) patterns of $LiNi_{0.975}Ti_{0.025}O_2$ powders preheated at 600°C for 16 h after milling for various times had peaks corresponding to the $LiNiO_2$ phase and peaks for Li_2CO_3 phase. The peaks for the $L1Ni_{0.975}Ti_{0.025}O_2$ powder milled for 28 h showed the highest intensities, indicating that the phases developed well. Therefore we chose 28 h for the ball milling time.

Figure 2 shows the XRD patterns of $LiNi_{0.975}Ti_{0.025}O_2$ powders calcined at 750, 800 and 850°C for 30 h in O_2 stream (after milling 28 h and preheating at 600°C for 16 h). They exhibit only the peaks corresponding to the $LiNiO_2$ phase. The intensities of the peaks increases and the splitting of 108 and 100 peaks become distinct as the calcining temperature rises.

Figure 3 shows the FE-SEM micrographs of $LiNi_{0.975}Ti_{0.025}O_2$ powders calcined at 750, 800 and 850°C for 30 h in O_2 stream (after milling 28 h and preheating at 600°C for 16 h). The

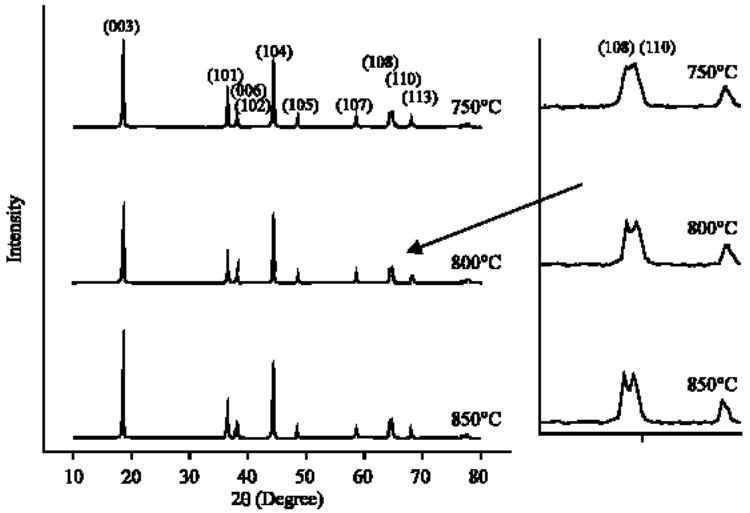

Fig. 2: XRD patterns of $LiNi_{0.975}Ti_{0.025}O_2$ powder calcined at 750, 800 and 850°C for 30 h in O_2 stream

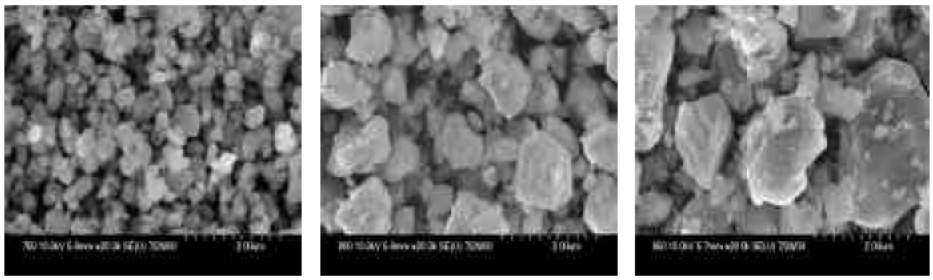

(a) (b) (c)

Fig. 3: FE-SEM micrographs of the $LiNi_{0.975}Ti_{0.025}O_2$ powder calcined at (a) 750°C, (b)800°C and (c)850°C for 30 h in O_2 stream

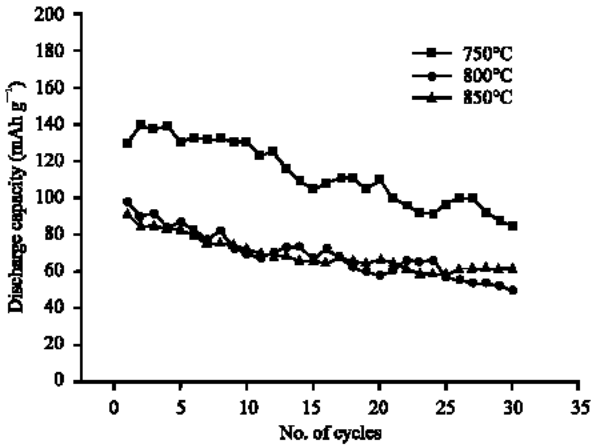

Fig. 4: Variations of discharge capacity at 0.1C with the number of cycles for $LiNi_{0.975}Ti_{0.025}O_2$ calcined at 750°C, 800°C and 850°C

Table 1: Lattice parameters and intensity ratio of 003 and 104 peaks, I_{003}/I_{104}, for $LiNi_{1-y}Ti_yO_2$ ($0 \le y \le 0.150$)

y in $LiNi_{1-y}Ti_yO_2$ ($0 \le y \le 0.150$)	a_{hex} (Å)	c_{hex} (Å)	c/a	I_{003}/I_{104}
0.000	2.873	14.225	4.951	1.195
0.012	2.875	14.195	4.937	1.258
0.025	2.876	14.194	4.935	1.133
0.050	2.877	14.182	4.930	1.076
0.100	2.876	14.153	4.921	1.000
0.150	2.884	14.154	4.907	0.949

particle size of the sample increases as the calcining temperature rises. The sample calcined at 750°C has the most homogeneous particle size.

Figure 4 shows the variations of discharge capacity at 0.1°C rate with the number of cycles (n) for $LiNi_{0.975}Ti_{0.025}O_2$ powders calcined at 750°C, 800°C and 850°C for 30 h in O_2 stream (after milling 28 h and preheating at 600°C for 16 h). The sample calcined at 750°C has the largest first discharge capacity and the similar cycling performance compared with the samples calcined at 800°C and 850°C. Therefore, we chose 750°C for the calcining temperature. $LiNi_{0.975}Ti_{0.025}O_2$ powder calcined at 750°C for 30 h in O_2 stream (after milling 28 h and preheating at 600°C for 16 h) showed relatively strong intensities of peaks in XRD pattern and had the smallest particles and the most homogeneous particle size compared with the samples calcined at 800°C and 850°C.

The XRD patterns of $LiNi_{1-y}Ti_yO_2$ powders calclined at 750°C for 30 h in O_2 stream (after milling 28 h and preheating at 600°C for 16 h) were analyzed to have the α-$NaFeO_2$ structure of the rhombohedral system (space group; $R\bar{3}m$).

Table 1 shows lattice parameters a,c and intensity ratio of 003 and 104 peaks, I_{003}/I_{104}, for $LiNi_{1-y}Ti_yO_2$ ($0 \le y \le 0.150$) calcined at 750°C for 30 h in O_2 stream. It is known that the intensity ratio of 003 and 104 peaks can be used to investigate the degree of cation (Li^+ and Ni^{2+}) mixing. When I_{003}/I_{104} is smaller than 1.2, the cation mixing occurs. On the other hand, when I_{003}/I_{104} is larger than 1.2, the composition of the sample is completely stoichiometric (Morales *et al*., 1990; Choi *et al*., 1996). The values of I_{003}/I_{104} for y = 0.100 and 0.150 compositions are 1.0 and 0.949, respectively, while those for y = 0.000, 0.012 and 0.025 are near 1.2. This indicates that the $LiNi_{1-y}Ti_yO_2$ (y = 0, 0.012 and 0.025) samples have the nearly stoichiometric compositions. It is also known that the splitting of two peaks 006 and 102 or 108 and 110 indicates the decrease in cation mixing. The splitting of 006 and 102 peaks occurs well for the samples with y = 0, 0.012 and 0.025, but it does not occur for the samples with y = 0.1 and 0.15. The splitting of 108 and 110 peaks occurs well for the samples with y = 0.000, 0.012, 0.025 and 0.050, but does not occur for the samples with y = 0.100 and 0.150.

The FE-SEM micrographs of the $LiNi_{1-y}Ti_yO_2$ powders calcined at 750°C for 30 h in O_2 stream showed that the particle size decreased as the value of y increased. All the samples except that with y = 0.000 exhibited relatively homogeneous particle size.

Figure 5 shows the voltage vs. discharge capacity curves of the first cycle for $LiNi_{1-y}Ti_yO_2$ (y = 0.000, 0.012, 0.025, 0.050, 0.100 and 0.150) calcined at 750°C for 30 h in O_2 stream. $LiNi_{0.975}Ti_{0.025}O_2$ has the largest first discharge capacity. The curves for y = 0.012 and y = 0.025 exhibit three distinct plateaus where phase transitions occur from hexagonal structure (H_3) to hexagonal structure (H_2), hexagonal structure (H_2) to monoclinic structure (M) and from monoclinic structure (M) to hexagonal structure (H_1).

Figure 6 shows the variations of discharge capacity at 0.1C rate with the number of cycle (n) for $LiNi_{1-y}Ti_yO_2$ calcined at 750°C for 30 h in O_2 stream. The cycling performance

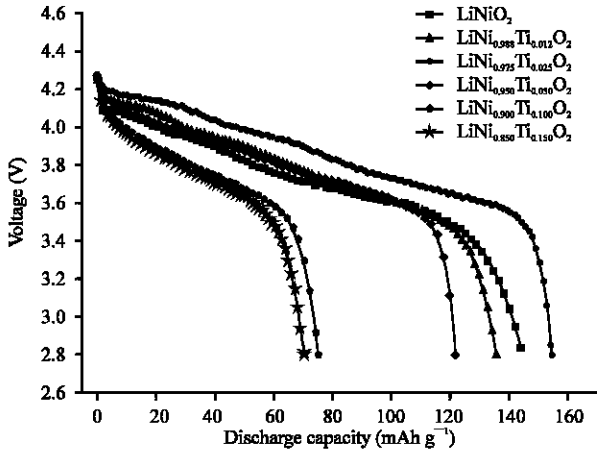

Fig. 5: Voltage vs. discharge capacity curves of the first cycle for $LiNi_{1-y}Ti_yO_2$ (y = 0.000, 0.012, 0.025, 0.050, 0.100 and 0.150)

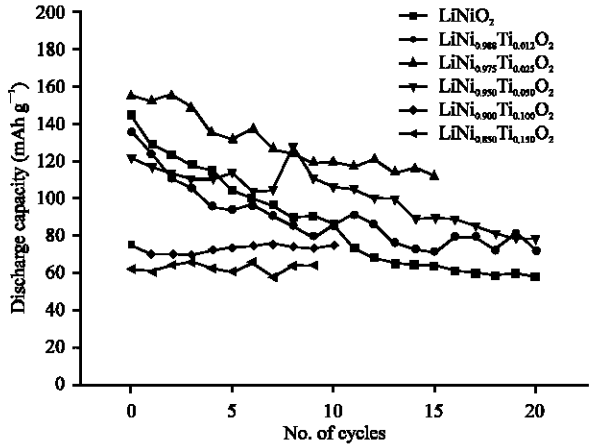

Fig. 6: Variations of discharge capacity with the number of cycles for $LiNi_{1-y}Ti_yO_2$; (a) y = 0.000 (b) y = 0.012 (c) y = 0.025 (d) y = 0.050 (e) y = 0.100 and (f) y = 0.150

(percentage of discharge capacity to the first discharge capacity) of $LiNiO_2$ at n = 10 is 60%. The cycling performance at n = 10 increases as the value of y increases. They are 63, 77 and 88%, respectively, for the samples with y = 0.012, 0.025 and 0.050. The samples with y = 0.100 and 0.150 have very small discharge capacities. When Ti is substituted for Ni in order to improve the cyclability of $LiNiO_2$, the composition $LiNi_{0.975}Ti_{0.025}O_2$ has the largest first discharge capacity 154.8 mAh g^{-1} and a relatively good cycling performance (77% at n = 10).

The above results show that the composition $LiNi_{0.975}Ti_{0.025}O_2$ has the best electrochemical properties among the compositions $LiNi_{1-y}Ti_yO_2$ (0 = y = 0.150). Instead of Ti in the compositions $LiNi_{0.975}Ti_{0.025}O_2$, Zn (with atomic value +2) and Al (with atomic value +3) were substituted.

Table 2: Lattice parameters and intensity ratio of 003 and 104 peaks, I_{003}/I_{104}, $LiNi_{0.975}M_{0.025}O_2$ (M = Zn^{2+}, Al^{3+} and Ti^{4+})

M in $LiNi_{0.975}M_{0.025}$	a_{hex} (Å)	c_{hex} (Å)	c/a	I_{003}/I_{104}
Zn^{2+}	2.875	14.150	4.921	1.379
Al^{3+}	2.870	14.151	4.930	1.400
Ti^{4+}	2.876	14.194	4.935	1.133

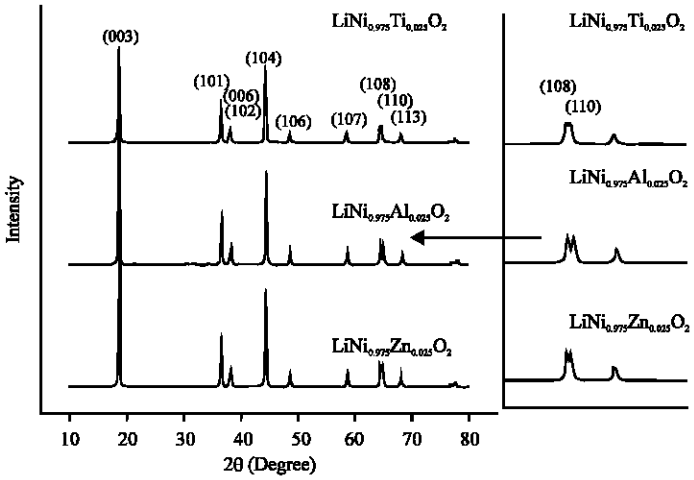

Fig. 7: XRD patterns of $LiNi_{0.975}M_{0.025}O_2$ (M = Zn^{2+}, Al^{3+} and Ti^{4+}) powders after calcining at 750°C for 30 h in O_2 stream

Figure 7 shows the XRD patterns of $LiNi_{0.975}M_{0.025}O_2$ (M = Zn^{2+}, Al^{3+} and Ti^{4+}) powders calcined at 750°C for 30 h in O_2 stream (after milling 28 h and preheating at 600°C for 16 h). All the samples were analyzed to have the α-$NaFeO_2$ structure of the rhombohedral system (space group; $R\bar{3}m$). The $LiNi_{0.975}Al_{0.025}O_2$ exhibits distinct splitting of 006 and 102 peaks and of 108 and 110 peaks, indicating very small amount of cation mixing. The $LiNi_{0.975}Zn_{0.025}O_2$ also shows relatively good splitting of 006 and 102 peaks and of 108 and 110 peaks.

Table 2 shows the lattice parameters and intensity ratio of 003 and 104 peaks, I_{003}/I_{104}, for $LiNi_{0.975}M_{0.025}O_2$ (M = Zn^{2+}, Al^{3+} and Ti^{4+}). The values of I_{003}/I_{104} for M = Zn^{2+} and Al^{3+} are 1.379 and 1.400, respectively. These values are quite large, indicting that the compositions of these samples are nearly stoichiometric.

Figure 8 shows the variations of hexagonal lattice parameters a, c and trigonal distortion c/a with M in $LiNi_{0.975}M_{0.025}O_2$ (M = Zn^{2+}, Al^{3+} and Ti^{4+}). The value of c/a increases as M varies from Zn^{2+} to Al^{3+} and then Ti^{4+}. This indicates that two-dimensional layered structure develops better as M varies from Zn^{2+} to Al^{3+} and then to Ti^{4+}.

The FE-SEM micrographs of the $LiNi_{0.975}M_{0.025}O_2$ (M = Zn^{2+}, Al^{3+} and Ti^{4+}) powders calcined at 750°C for 30 h in O_2 stream showed that the samples with M = Zn^{2+} and Al^{3+} had small particles and large particles. As M varies from Zn^{2+} to Al^{3+} and then to Ti^{4+}, the particles became smaller. $LiNi_{0.975}Ti_{0.025}O_2$ had particles with similar sizes.

Figure 9 shows the voltage vs. discharge capacity curves of the first cycle for $LiNi_{0.975}M_{0.025}O_2$ (M = Zn^{2+}, Al^{3+} and Ti^{4+}). $LiNi_{0.975}Ti_{0.025}O_2$ has the curve showing the most distinct plateaus. The voltage of the plateau corresponding to the phase transition

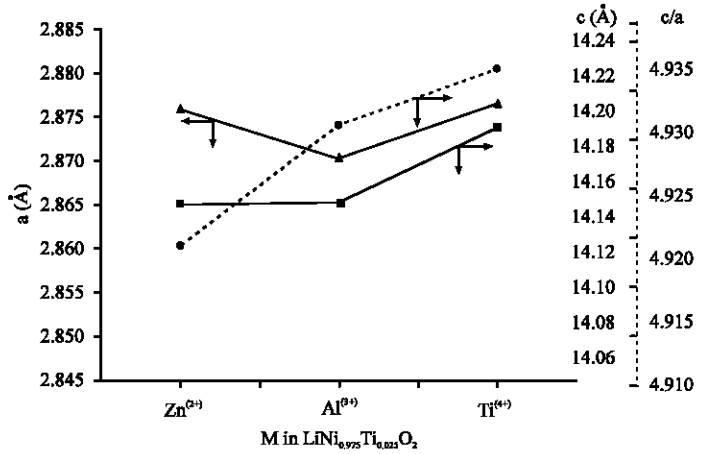

Fig. 8: Variations of hexagonal lattice parameters a, c and trigonal distortion c/a with M in $LiNi_{0.975}M_{0.025}O_2$ ($M = Zn^{2+}$, Al^{3+} and Ti^{4+})

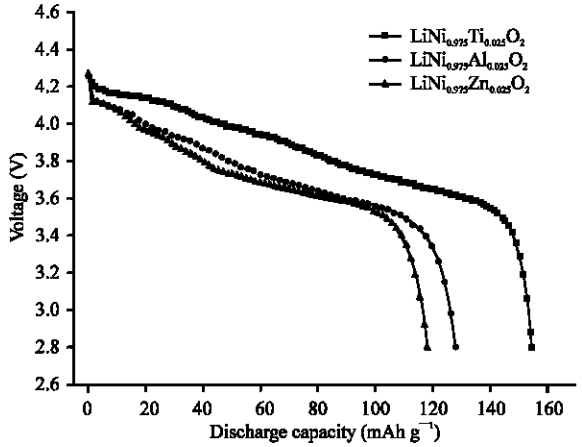

Fig. 9: Voltage vs. discharge capacity curves of the first cycle for $LiNi_{0.975}M_{0.025}O_2$ ($M = Zn^{2+}$, Al^{3+} and Ti^{4+})

from M to H_1 increases as M varies from Zn^{2+} to Al^{3+} and then to Ti^{4+}. They are 3.68, 3.69 and 3.75V, respectively.

Figure 10 shows the variations of discharge capacity at 0.1C rate with the number of cycles (n) for $LiNi_{0.975}M_{0.025}O_2$ ($M = Zn^{2+}$, Al^{3+} and Ti^{4+}). $LiNi_{0.975}Ti_{0.025}O_2$ has the largest first discharge capacity (154.8mAhg^{-1}), followed in order by $LiNi_{0.975}Al_{0.025}O_2$ (128.5mAhg^{-1}) and $LiNi_{0.975}Zn_{0.025}O_2$ (118.6mAhg^{-1}). The cycling performances at n = 10 are 77%, 98% and 85%, respectively, for $LiNi_{0.975}M_{0.025}O_2$ ($M = Zn^{2+}$, Al^{3+} and Ti^{4+}). These results agree well to the reported data. It is known that the substitution of a non-transition element Al improves cyclabiltiy (Ohzuku *et al*., 1993; Fey *et al*., 2003; Song and Lee, 2002) and the substitution of Zn improves cyclability a little but unsatisfactorily (Fey *et al*., 2003; 2002). $LiNi_{0.975}Ti_{0.025}O_2$ has the largest first discharge capacity and a relatively good cycling performance.

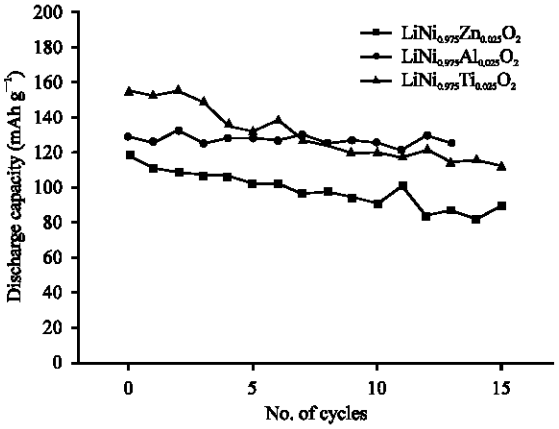

Fig. 10: Variations of discharge capacity with the number of cycles for $LiNi_{0.975}M_{0.025}O_2$ (M = Zn^{2+}, Al^{3+} and Ti^{4+})

Conclusions

The optimum condition to synthesize a cathode material $LiNi_{0.975}Ti_{0.025}O_2$ is milling for 28 h and then preheating at 600°C for 16 h and finally calcining at 750°C for 30 h O_2 stream. $LiNi_{1-y}Ti_yO_2$ ($0 \le y \le 0.150$) synthesized under this optimum condition have the α-$NaFeO_2$ structure of the rhombohedral system (space group; $R\bar{3}m$). The values of I_{003}/I_{104} for y = 0.000, 0.012 and 0.025 are near 1.2, indicating these samples have the phase with the nearly stoichiometric composition. The samples with y = 0, 0.012 and 0.025 show good splitting of 006 and 102 peaks and of 108 and 110 peaks, indicating the decrease in cation mixing. The particle size decreases as the value of y increases. All the samples except that with y = 0.000 exhibit relatively homogeneous particle size. The voltage vs. discharge capacity curves for y = 0.012 and y = 0.025 exhibit three distinct plateaus corresponding to phase transitions. Among $LiNi_{1-y}Ti_yO_2$ ($0 = y = 0.150$), $LiNi_{0.975}Ti_{0.025}O_2$ has the largest first discharge capacity 154.8mAh g^{-1} and the relatively good cycling performance (77% at n = 10).

Electrochemical studies of $LiNi_{0.975}M_{0.025}O_2$ (M = Zn^{2+}, Al^{3+} and Ti^{4+}) show that the plateaus in the voltage vs. discharge capacity curve become more distinct and the voltage of the plateau corresponding to the phase transition from M to H_1 increases as M varies from Zn^{2+} to Al^{3+} and then to Ti^{4+}. $LiNi_{0.975}Ti_{0.025}O_2$ has the largest first discharge capacity and a relatively good cycling performance compared with $LiNi_{0.975}M_{0.025}O_2$ (M = Zn^{2+} and Al^{3+}). This sample has the largest value of c/a and the smallest particles. $LiNi_{0.975}Al_{0.025}O_2$ has the best cycling performance (98% at n = 10).

References

Alcantara, R., P. Lavela, J.L. Tirado, R. Stoyanova and E. Zhecheva, 1997. Structure and electrochemical properties of boron-doped $LiCoO_2$. J. Solid State Chem., 134: 265-273.

Ahn, D.S. and M.Y. Song, 2000. Variatinns of the electrochemica properties of $LiMn_2O_4$ with synthesis conditions. J. Electrochem. Soc., 147: 874-879.

Broussely, M., 1990. Recent developments on lithium ion batteries at SAFT. J. Power Sources, 81-82: 140-143.

Caurant, D., N. Baffier, B. Garcia and J.P. Pereira-Ramos, 1996. Synthesis by a soft chemistry route and characterization of $LiNi_xCo_{1-x}O_2$ (0×1) cathode materials. Solid State Ionics, 91: 45-54.

Choi, Y.M., S.I. Pyun and S.I. Moon, 1996. Effects of cation mixing on the electrochemical lithium intercalation reaction into porous Li_1 - $\delta Ni_{1-y}Co_yO_2$ electrodes. Solid State Ionics, 89: 43-52.

Dahn, J.R., U. von Sacken and C.A. Michal, 1990. Structure and electrochemistry of $Li_{1+y}NiO_2$ and a new Li_2NiO_2 phase with the Ni $(OH)_2$ structure. Solid State Ionics, 44: 87-97.

Dahn, J.R., U. von Sacken, M.W. Juzkow and H. Al-Janaby, 1991. Rechargeable $LiNiO_2$/CarbonCells. J. Electrochem. Soc., 138: 2207-2212.

Ebner, W., D. Fouchard and L. Xie, 1994. The $LiNiO_2$/carbon lithium-ion battery. Solid State Ionics, 69: 238-256.

Fey, G.T.K., J.G. Chen, V. Subramanian and T. Osaka, 2002. Preparation and electrochemical properties of Zn-doped $LiNi_{0.8}Co_{0.2}O_2$. J. Power Sources, 112: 384-394.

Fey, G.T.K., J.G. Chen and V. Subramanian, 2003. Electroanalytical and thermal stability studies of multi-doped lithium nickel cobalt oxides. J. Power Sources, 119-121: 658-663.

Gao, T., M.V. Yakovleva and W.B. Ebner, 1998. Novel $LiNi_{1-x}Ti_{x/2}Mg_{x/2}O_2$ Compounds as cathode materials for safer lithium-ion batteries. Electrochem. Solid-state Letters, 1:117.

Kim, J. and K. Amine, 2002. A comparative study on the substitution of divalent, trivalent and tetravalent metal ions in $LiNi_{1-x}M_xO_2$ ($M = Cu^{2+}$, Al^{3+} and Ti^{4+}). J. Power Sources, 104: 33-39.

Morales, J., C. Peres-Vicente and J.L.Trado, 1990. Cation distribution and chemical deintercalation of $Li_{1-x}Ni_{1+x}O_2$. Mat. Res. Bull., 25: 623-630.

Marini, A., V. Massarotti, V. Berbenni, D. Capsoni, R. Riccardi, E. Antolini and B. Passalacqua, 1991. On the thermal stability and defect structure of the solid solution $Li_xNi_{1-x}O$. Solid State Ionics, 45: 143-155.

Nishida, Y., K. Nakane and T. Stoh, 1997. Synthesis and properties of gallium-doped $LiNiO_2$ as the cathode material for lithium secondary batteries. J. Power Sources, 68: 561-564.

Ohzuku, T., A. Ueda and M. Nagayama, 1993. Electrochemistry and structural chemistry of $LiNiO_2$ (Rm) for 4 volt secondary lithium cells. J. Electrochem. Soc., 140: 1862.

Ozawa, K., 1994. Lithium-ion rechargeable batteries with $LiCoO_2$ and carbon electrodes: The $LiCoO_2$/C system. Solid State Ionics, 69: 212-221.

Peng, Z.S., C.R. Wan and C.Y. Jiang, 1998. Synthesis by sol-gel process and characterization of $LiCoO_2$ cathode materials. J. Power Sources, 72: 215-220.

Song, M.Y. and D.S. Ahn, 1998. On the capacity deterioration of spinel phase $LiMn_2O_4$with cycling around 4 V. Solid State Ionics, 112: 21-24.

Song, M.Y., D.S. Ahn and H.R. Park, 1999. Capacity fading of spinel phase $LiMn_2O_4$ with cycling. J. Power Sources, 83: 57-60.

Song, M.Y. and R. Lee, 2002. Synthesis by sol-gel method and electrochemical properties of $LiNiO_2$ cathode material for lithium secondary battery. J. Power Sources, 111: 97-103.

Tarascon, J.M., E. Wang, F.K. Shokoohi, W.R. Mckinnon and S. Colson, 1991. The Spinel Phase of $LiMn_2O_4$ as a Cathode in Secondary Lithium Cells. J. Electrochem. Soc., 138: 2859-2864.